Embedding dynamics for round-off errors near a periodic orbit

J. H. Lowenstein and F. Vivaldi†

Dept. of Physics, New York University, 2 Washington Place,
New York, NY 10003, USA
†School of Mathematical Sciences, Queen Mary and Westfield College,
London E1 4NS, UK

Abstract

We study the propagation of round-off errors near the periodic orbits of a linear map conjugate to a planar rotation with rational rotation number. We embed the two-dimensional discrete phase space (a lattice) in a higher-dimensional torus, where points sharing the same round-off error are uniformly distributed within finitely many convex polyhedra. The embedding dynamics is linear and discontinuous, with algebraic integer coefficients. This representation affords efficient algorithms for classifying and computing the orbits and their densities, which we apply to the case of rational rotation number with denominator 7, corresponding to certain algebraic integers of degree three. We provide evidence that the hierarchical arrangement of orbits previously detected in quadratic cases [7] disappears, and that the growth of the number of orbits with the period is algebraic.

1 Introduction

The study of round-off errors in computer representations of dynamical systems has attracted considerable attention in recent years, due to its theoretical and practical significance, and its rich dynamics. Within the context of spatial discretizations of symplectic mappings, of importance are the linear planar rotations, where the continuum dynamics is regular and well-understood, and where round-off errors can be studied in isolation from other dynamical phenomena [2, 5, 11, 7, 12, 9, 3].

In this paper we consider the case of *uniform* discretization of coordinates (as opposed to the floating-point discretization), with the requirement that the discrete mapping remain invertible after discretization. In this setting one speaks of *hamiltonian* round-off errors.

Systems of this type naturally involve the study of discontinuous affine transformations of the torus, which have appeared in a variety of contexts, ranging from polygonal dual billiards to digital filters (see [1] and references therein). The properties of such systems are still far from understood theoretically, and notoriously difficult to approach numerically. Therefore it seems appropriate to develop a geometrical environment suitable for the algorithmic side of the problem, which is the aim of the present work.

We study hamiltonian round-off errors around elliptic-type motions with rational rotation number p/q (p and q coprime). Specifically, we consider the planar map [11, 7, 9, 3]

$$\Psi\begin{pmatrix}x\\y\end{pmatrix}=\begin{pmatrix}\lambda & -1\\ 1 & 0\end{pmatrix}\begin{pmatrix}x\\y\end{pmatrix}=\begin{pmatrix}\lambda x-y\\ x\end{pmatrix};\qquad |\lambda|<2 \tag{1}$$

where the rotation number is related to the trace λ by the equation

$$\lambda = 2\cos(2\pi p/q). \tag{2}$$

We discretize the phase space $\mathbf{R}^2$ of (1) to the lattice $\mathbf{Z}^2$ as follows:

$$\Phi\begin{pmatrix}x\\y\end{pmatrix}=\begin{pmatrix}\lfloor\lambda x\rfloor-y\\ x\end{pmatrix}=\Psi\begin{pmatrix}x\\ y+\epsilon(x)\end{pmatrix} \tag{3}$$

where $\lfloor\cdot\rfloor$ is the floor function and

$$\epsilon(x)=\lambda x-\lfloor\lambda x\rfloor\qquad \epsilon(x+\tau)=\epsilon(x),\qquad \tau=\lambda^{-1}. \tag{4}$$

One verifies that the discrete mapping Φ is still invertible (note that the analogous discretization of the Jordan form of (1) is not). In the above representation, the discretization length is fixed, and the limit of small discretization corresponds to motions near infinity.

From equation (2) one can show that for $q>2$ the parameter λ is an *algebraic integer* [1] of degree $\phi(q)/2$, where ϕ is the Euler's function, which counts the number of integers less than q and coprime to it (see, e.g., [10], Chapter 2). For $q=3,4,6$, λ is a rational integer, and so there are no round-off errors. The simplest non-trivial

[1] a root of an irreducible polynomial with integer coefficients and unit leading coefficient

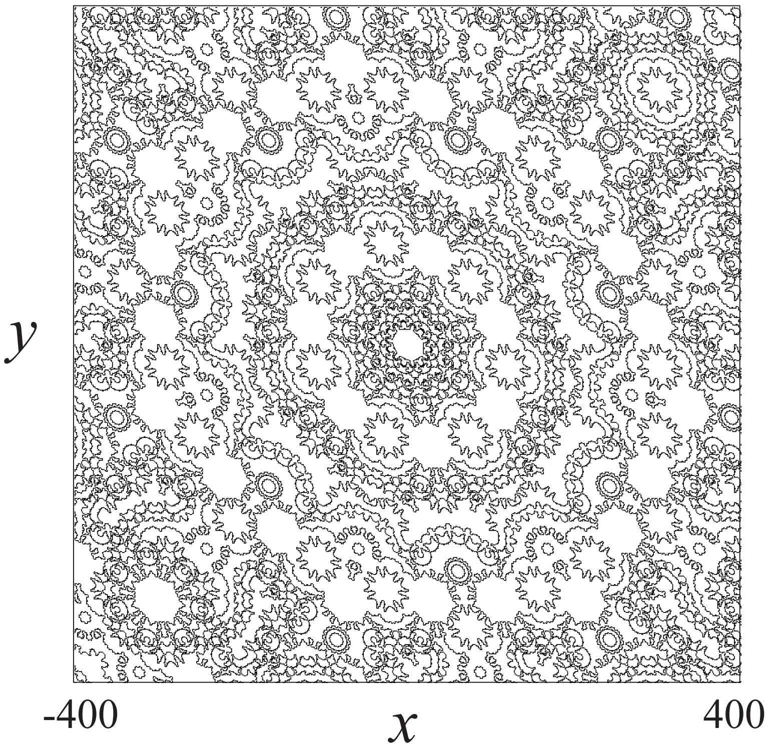

Figure 1: Round-off orbits for the rotation number 2/7. We display all orbits in the region $-400 \le x, y \le 400$, whose periods are no less than 200. They are all periodic.

cases are $q = 5, 8, 10, 12$, where λ is a quadratic integer (the case $p/q = 1/5$ was studied in [7, 9]), while $q = 7$ is the smallest value of q for which λ has degree three. In general, each degree corresponds to finitely many values of q.

The cumulative round-off error after one period will be characterized by the *discrete vector field* associated with the mapping Φ, defined as

$$\mathbf{v} : \mathbf{Z}^2 \mapsto \mathbf{Z}^2 \qquad\qquad \mathbf{z} \mapsto \Phi^q(\mathbf{z}) - \mathbf{z}. \tag{5}$$

The round-off orbits are the 'integral curves' of $\mathbf{v}$, some of which are displayed in figure 1 for the rotation number $p/q = 2/7$.

The points of vanishing vector field correspond to initial conditions where the round-off errors cancel out, and the discrete mapping has the same periodicity of the continuum one. For all other initial conditions one finds (numerically) that the round-off orbits are periodic, that is, that no orbit escapes to infinity. The finer the discretization, i.e., the further one is from the origin, the longer the observed maximal periods.

Since at each iteration the magnitude of the round-off error is bounded, the vector field (5) can assume only finitely many values, yielding a natural symbolic dynamics. Furthermore, if the lattice $\mathbf{Z}^2$ is equipped with the Φ-invariant (non countably additive) *density* measure, one finds that each level set of the vector field is measurable, and consists of points scattered quasi-periodically on the lattice. This observation leads to a probabilistic description of round-off errors. The orbits with the same symbolic sequence are regrouped by translational invariance into equivalence classes, which are quasi-periodic sets on $\mathbf{Z}^2$. The contribution of each orbit class to the round-off error depends on its measure, whose computation is our main concern.

The main theoretical results of this paper are theorems 1 and 2 (see sections 2 and 3). These theorems state that the two-dimensional discrete phase space $\mathbf{Z}^2$ can be embedded densely and uniformly in the *local phase space* Ω, which is a higher-dimensional torus (hypercube). Locally, the dynamics is represented by a linear mapping with coefficients in the maximal real subfield of the qth cyclotomic field. The orbits in $\mathbf{Z}^2$ sharing the same symbolic code correspond to convex polyhedra, and the uniformity of the embedding implies that the normalized volume of the polyhedra gives the phase space density of the corresponding orbits.

The probabilistic description of round-off errors requires knowledge of the probability $P(\mathbf{z}, t)$ that a randomly chosen point in $\mathbf{Z}^2$ be displaced by an integer vector $\mathbf{z}$ after t iteration of the map Φ^q. Such probability is a finite sum over all t-elements sequences of vector field steps leading to $\mathbf{z}$, each weighted by its measure. As the latter is an algebraic number, $P(\mathbf{z}, t)$ can be computed exactly (i.e., symbolically). In practice, these computations become manageable only by summing over periodic orbits, and in sections 3 and 4 we exploit the above theorems to derive explicit algorithms for computing periodic orbits and their probabilities.

In section 5 we implement our algorithm to the analysis of the rotation numbers 1/7 and 2/7, where the trace of the map Ψ is an algebraic integer of degree three. We compute all orbits of period up to 21,000 and 49,000, respectively, and the corresponding densities, and the round-off errors probability distribution. We find no evidence of the hierarchical organization into finitely many families which characterizes the quadratic cases studied previously [7] (see also [1]). These results suggest

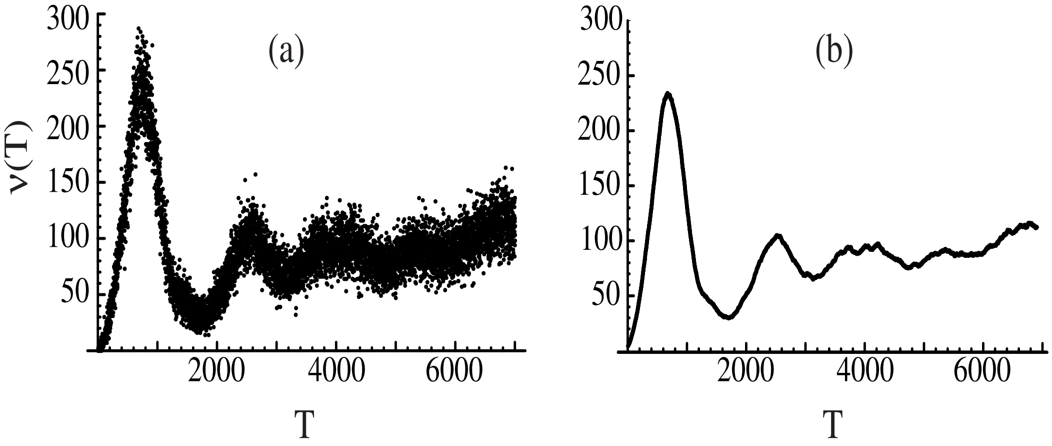

Figure 2: The number $\nu(T)$ of orbit classes as a function of the period T, for the rotation number $2/7$: (a) all the data; (b) average over the interval $[T-50, T+50)$.

the existence of an infinite number of distinct periodic orbit classes, with unbounded period, and which account for the full measure. We have found no escape orbits, but there exist orbit classes having zero measure, forming a sequence of isolated annular orbits (see figure 3b). The computation of the number of orbit classes as the function of their period (figure 2) is consistent with an algebraic growth with a small fractional exponent, but is also plagued by a very slow convergence, which seems typical in this class of problems.

One of us (FV) would like to thank Ilya Goldshied for a useful discussion on uniform distribution.

2 Localization

In this section we embed the two-dimensional discrete phase space $\mathbf{Z}^2$ in a higher-dimensional torus (hypercube), where the dynamics takes on a particularly simple form.

Let the rotation number be p/q, with $q > 2$. The parameter λ given by equation (2) is a root of the irreducible polynomial $h_q(X)$, defined by

$$h_q(X + X^{-1}) \;=\; H_q(X)\, X^{-\phi(q)/2}. \tag{6}$$

Here ϕ is the Euler's totient function, and $H_q(X)$ is the qth cyclotomic polynomial

$$H_q(X) = \prod_{d|q} (X^{q/d} - 1)^{\mu(d)}$$

where μ is the Möbius function ([10], chapter 2). The roots of $H_q(X)$ are the primitive qth roots of unity: in particular, if $\eta = e^{2\pi i p/q}$, then $H_q(\eta) = 0$, whence, from (6) one verifies that $h_q(\lambda) = h_q(\eta + \eta^{-1}) = 0$.

We shall denote by $\mathcal{M}[a, b, \ldots]$ the set of all integral linear combinations of arbitrary vectors $a, b, \ldots$. Thus $\mathcal{M}$ is a vector space where the 'scalars' are integers (a $\mathbf{Z}$-module, in algebraic jargon). The module $\mathcal{M}[1, \lambda, \lambda^2, \ldots, \lambda^{\phi(q)/2-1}]$ is also the ring of integers in the algebraic number field $\mathbf{Q}(\lambda)$, and for it we shall use the shorthand notation $\mathbf{Z}[\lambda]$. ($\mathbf{Q}(\lambda)$ is obtained by adjoining λ to the rationals, resulting in a $\phi(q)/2$-dimensional vector space over $\mathbf{Q}$.)

The algebraic number τ characterizing the periodicity of the round-off function (4) is a root of the irreducible polynomial

$$X^{\phi(q)/2} h_q(1/X)$$

which has integer coefficients but which is not necessarily monic, i.e., τ may not be an algebraic integer.

Alongside an orbit $\{(x_t, y_t),\, t = 0, 1, \ldots\}$ of (3), we introduce the sequence of normalized round-off errors

$$\zeta_t = \tau \epsilon(x_t) \,\in\, \mathcal{M}[1, \tau] \cap \mathcal{I}, \qquad t = 0, 1, \ldots, \tag{7}$$

where

$$\mathcal{I} = \begin{cases} [0, \tau), & \tau > 0 \\ (\tau, 0], & \tau < 0 \end{cases} \tag{8}$$

From (3) and (4) we find the recursion formula

$$\zeta_{t+2} = -\zeta_t + m_{t+1} - \tau\,(m_t + m_{t+2}), \qquad m_t = \lfloor \lambda\, x_t \rfloor \tag{9}$$

with initial conditions

$$\zeta_0 = x_0 - \tau\, m_0, \qquad \zeta_1 = y_0 + m_0 - \tau\, m_1,$$

which suggests the introduction of the following set of $\phi(q)$ vectors in $\mathbf{R}^d$, where

$$d = \phi(q) - 2 \tag{10}$$

(the rationale behind the choice of d will soon become clear)

$$\begin{array}{rcl}
\mathbf{e}^{(-2)} &=& (\ \ 0, -1, \ \ 0, \ \ 1, \ \ 0, -1, \dots) \\
\mathbf{e}^{(-1)} &=& (\ \ 1, \ \ 0, -1, \ \ 0, \ \ 1, \ \ 0, \dots) \\
\mathbf{e}^{(0)} &=& (-\tau, \ \ 1, \ \ 0, -1, \ \ 0, \ \ 1, \dots) \\
\mathbf{e}^{(1)} &=& (\ \ 0, -\tau, \ \ 1, \ \ 0, -1, \ \ 0, \dots) \\
\mathbf{e}^{(2)} &=& (\ \ 0, \ \ 0, -\tau, \ \ 1, \ \ 0, -1, \dots) \\
& \vdots & \\
\mathbf{e}^{(d-1)} &=& (\ \ 0, \ \ 0, \ \ \dots \ \ 0, -\tau)
\end{array}$$

that is, the $\mathbf{e}$-vectors have components

$$\mathbf{e}_k^{(t)} = \begin{cases} 0 & k < t \\ -\tau & k = t \\ \delta_{k-t-1} & k > t \end{cases}, \qquad -2 \le t \le d-1, \qquad 0 \le k \le d-1, \tag{11}$$

where

$$\delta_i = \begin{cases} (-1)^{i/2} & i \text{ even} \\ 0 & i \text{ odd}. \end{cases} \tag{12}$$

If we let $\zeta = (\zeta_0, \dots, \zeta_{d-1})$ be delay coordinates in $\Omega = \mathcal{I}^d$, the recursion (9) gives the representation

$$\zeta = x\,\mathbf{e}^{(-1)} + y\,\mathbf{e}^{(-2)} + \sum_{t=0}^{d-1} m_t\,\mathbf{e}^{(t)} \tag{13}$$

where we have written x, and y for x_0 and y_0 and where the coefficients m_t depend on x and y via (9). The above equation defines a mapping $\mathcal{E} : \mathbf{Z}^2 \mapsto \Omega$.

Before stating the main result of this section, we recall some standard definitions. The *companion matrix* of the polynomial

$$f(X) = c_0 + c_1\,X + \dots + c_{d-1}\,X^{d-1} + X^d$$

is given by [6]

$$C = \begin{pmatrix} 0 & 1 & 0 & \cdots & 0 \\ 0 & 0 & 1 & \cdots & 0 \\ \vdots & \vdots & \ddots & \ddots & \vdots \\ 0 & 0 & 0 & \cdots & 1 \\ -c_0 & -c_1 & -c_2 & \cdots & -c_{d-1} \end{pmatrix} \tag{14}$$

One verifies that C has characteristic polynomial $f(X)$.

The *density* of a set $A \subseteq \mathbf{Z}^2$ is defined as

$$\lim_{n\to\infty} \frac{1}{(2n)^2} \#\{(x,y) \in A;\, |x|,|y| < |n|\}. \tag{15}$$

if the limit exists.

The main result of this section is the following

Theorem 1 *The mapping (13) defines a dense and uniform embedding of $\mathbf{Z}^2$ into Ω. The conjugate mapping $\Phi^* = \mathcal{E} \circ \Phi \circ \mathcal{E}^{-1}$ extends to a dynamical system on Ω given by*

$$\zeta \mapsto C \cdot \zeta \pmod{\tau}, \tag{16}$$

where C is the companion matrix of the polynomial

$$f(X) = \frac{H_q(X)}{X^2 - \lambda X + 1} \tag{17}$$

and H_q is the qth cyclotomic polynomial.

The modular operation in (16) is confined to the last co-ordinate, since all other coordinates are permuted cyclically. This introduces a discontinuity in the dynamics.

Proof of theorem 1. The roots of $f(X)$ are all the primitive q-th roots of unity, with the exception of the conjugate elements η and η^{-1}, which are the roots of the denominator of the right hand side of (17). By construction, $f(X)$ is reflexive: $f(X) = X^d f(1/X)$, being the ratio of two reflexive polynomials. The coefficients of $f(X)$ belong to $\mathbf{Z}[\lambda]$ and are symmetrical: $c_0 = 1$ and $c_k = c_{d-k}$, for $k = 1, \ldots, d-1$, and since $\Phi^*(\Omega)$ still tiles $\mathbf{R}^d$ under translation, the mapping Φ^* defines a bijection of Ω.

Because the ζ are delay coordinates, the time-evolution induces a left shift of the first $d-1$ components, which accounts for the first $d-1$ rows of the matrix C. As to the last row, we rewrite (17) as

$$(X^2 - \lambda X + 1) \sum_{k=0}^{d} c_k X^k = H_q(X) \stackrel{\text{def}}{=} \sum_{k=0}^{d+2} r_k X^k. \tag{18}$$

Matching coefficients of equal powers of X, one finds the recursion formula

$$c_{-1}=0; \qquad c_0=1; \qquad c_k=\lambda\, c_{k-1}-c_{k-2}+r_k, \quad k\geq 1. \tag{19}$$

Let $\mathbf{c}=(c_0,\ldots,c_{d-1})$. The above formula together with the reflexivity of $f(X)$ gives the scalar product formulae

$$\begin{aligned}
\mathbf{c}\cdot\mathbf{e}^{(d-1)} &= -1-\tau\, r_1 \\
\mathbf{c}\cdot\mathbf{e}^{(d-2)} &= \tau\,(1-r_2) \\
\mathbf{c}\cdot\mathbf{e}^{(t-2)} &= -\tau\, r_t-\mathbf{c}\cdot\mathbf{e}^{(t)}, \qquad t=0,\ldots,d-1.
\end{aligned} \tag{20}$$

This shows that $\mathbf{c}\cdot\mathbf{e}^{(t)}\in\mathcal{M}[1,\tau]$ for all t, and since

$$\mathbf{c}\cdot\zeta=x_0\,\mathbf{c}\cdot\mathbf{e}^{(-1)}+y_0\,\mathbf{c}\cdot\mathbf{e}^{(-2)}+\sum_{t=0}^{d-1} m_t\,\mathbf{c}\cdot\mathbf{e}^{(t)}$$

we find that C leaves Ω invariant. Moreover, (20) also gives

$$\mathbf{c}\cdot\mathbf{e}^{(d-2i+1)}\equiv(-1)^i\,(\mathrm{mod}\ \tau) \qquad \mathbf{c}\cdot\mathbf{e}^{(d-2i)}\equiv 0\,(\mathrm{mod}\ \tau) \qquad i=1,2,\ldots \tag{21}$$

and recalling that d is even (cf. (10)), we have

$$\begin{aligned}
-\mathbf{c}\cdot\zeta &\equiv m_{d-1}-m_{d-3}+m_{d-5}-\cdots+(-1)^{d/2}(-m_1+x_0)\,(\mathrm{mod}\ \tau) \\
&\equiv \zeta_d\,(\mathrm{mod}\ \tau).
\end{aligned}$$

This proves that Φ^* is represented by (16) in Ω.

Next we show that $\mathcal{E}(\mathbf{Z}^2)$ is uniformly distributed in Ω. We note that the d vectors $\mathbf{e}^{(0)},\ldots,\mathbf{e}^{(d-1)}$ are linearly independent and lie in $\mathcal{M}[1,\tau]^d$. They generate the d-dimensional lattice

$$\mathbf{M}=\mathcal{M}[\mathbf{e}^{(0)},\,\ldots,\,\mathbf{e}^{(d-1)}]$$

Letting

$$a_{-1}=0; \qquad a_0=\lambda; \qquad a_{k+1}=\lambda\, a_k-a_{k-1}, \quad k\in\mathbf{Z}$$

one finds

$$\mathbf{e}^{(-2)}=\sum_{k=0}^{d-1} a_{k-1}\mathbf{e}^{(k)} \qquad \mathbf{e}^{(-1)}=-\sum_{k=0}^{d-1} a_k\mathbf{e}^{(k)}.$$

This shows that

$$\mathcal{E}(x,y) \equiv \sum_{k=0}^{d-1} f_k(x,y)\,\mathbf{e}^{(k)} \pmod{\mathbf{M}}, \qquad f_k(x,y) = -x\,a_k + y\,a_{k-1}.$$

Let $\mathcal{L} \subset \mathbf{R}^d$ be the fundamental parallelogram of the lattice $\mathbf{M}$. Because the f_k are homogeneous forms in x and y, the image of $\mathbf{Z}^2$ will be uniformly distributed in $\mathcal{L}$ provided that the only set of integers $s_0, \ldots, s_{d-1}$ such that

$$s_0 f_0(x,y) + \cdots + s_{d-1} f_{d-1}(x,y) = -N\,x + M\,y \tag{22}$$

with integer coefficients M and N, is $s_0 = \cdots = s_{d-1} = 0$ ([4], page 64).

The $a_k(\lambda)$ are integral polynomials in λ of degree $|k+1|$, and since the degree of h_q is $d/2+1$ (cf. (6) and (10)), as long as $-d/2-1 \leq k < d/2$, the powers λ are independent over $\mathbf{Q}$, so the integrality condition must be imposed separately on each coefficient. Writing, for all k and l

$$a_{k-l} = P_{l+1}\,a_k - P_l\,a_{k+1} \tag{23}$$

we find

$$P_{-1} = -1 \qquad P_0 = 0 \qquad\qquad P_{l+1} = \lambda\,P_l - P_{l-1} \tag{24}$$

so that P_l is a polynonomial in λ of degree $l-1$ (for $l \geq 1$). With reference to (22), we now let

$$N \;=\; s_{d-1}\,a_{d-1} + \cdots + s_0\,a_0 \tag{25}$$

$$M \;=\; s_{d-1}\,a_{d-2} + \cdots + s_0\,a_{-1} \tag{26}$$

where M and N are integers, and obtain, using (23)

$$P_l\,M - P_{l-1}\,N \;=\; s_{d-1}\,a_{d-1-l} + s_{d-2}\,a_{d-2-l} + \cdots + s_1\,a_{1-l} - P_{l-1}\,s_0\,a_0$$
$$l = 0, \ldots, d/2. \tag{27}$$

(For $l = 0, 1$ the above reduce to (25) and (26), respectively.) For $l = d/2$, the LHS of (27) has degree $d/2-1$, while the RHS has degree $d/2$. This implies $s_{d-1} = 0$. Substituting this back into the preceding equation kills s_{d-2} and s_{d-3}. A simple induction then shows that the lth equation (27) kills the coefficients s_{2l} and s_{2l-1}, while the first equation ($l = 0$) kills s_0.

This proves uniform distribution in $\mathcal{L}$, whence in Ω, which is obtained from $\mathcal{L}$ by a linear non-singular transformation. The conjugate map $\Phi^* = \mathcal{E} \circ \Phi \circ \mathcal{E}^{-1}$ then admits a unique continuous extension to Ω.

□

3 Partition of Ω into convex polyhedra

The principal advantage of representing the round-off map in the local phase space is that it groups together, within convex polyhedral regions, quasiperiodically distributed points of $\mathbf{Z}^2$ with identical dynamical trajectories. Conveniently, the density of the points in the quasi-periodic set is proportional to the volume of the corresponding polyhedron. The basis for this localization of orbits is the following theorem, which associates level sets of the vector field with certain convex polyhedra in Ω.

Theorem 2 *The map Φ^* of Theorem 1 induces a finite partition*

$$\Omega = \bigcup_{\mathbf{n}} \Omega_{\mathbf{n}} \qquad \mathbf{n} = (n_0, \ldots, n_{q-d-1}) \in \mathbf{Z}^{q-d}, \tag{28}$$

where $\Omega_{\mathbf{n}}$ is a convex polyhedron of dimension $\leq d$. All points $\mathbf{z} \in \mathbf{Z}^2$ such that $\mathcal{E}(\mathbf{z}) \in \Omega_{\mathbf{n}}$ have the same value of the vector field (5), and their density is equal to the normalized volume of the polyhedron.

In what follows, all convex polyhedra will be specified by q pairs of inequalities determined by the conditions

$$\mathbf{u}^{(i)} \cdot \zeta \in \mathcal{I}^{(i)}, \qquad i = 0, \ldots, q-1, \tag{29}$$

where

$$\mathbf{u}^{(0)} = (1, 0, \cdots, 0), \qquad \mathbf{u}^{(i)} = C' \mathbf{u}^{(i-1)}, \tag{30}$$

with C' denoting the transpose of C, and $\mathcal{I}^{(i)}$ is a half-open interval with endpoints in $\mathbf{Q}(\lambda)$, to be defined below. The interval is closed on the left (resp. right) for $\lambda > 0$ (resp. $\lambda < 0$). In the course of the proof, we shall derive various formulae related to equation (28), which we collect in the following

Proposition 3.1 *Each polyhedron $\Omega_{\mathbf{n}}$ in (28) is of the form (29), with $\mathcal{I}^{(i)}$ given by*

$$\begin{array}{ll} \mathcal{I}^{(i)} = \mathcal{I}, & i = 0, \ldots, d-1 \\ \mathcal{I}^{(d+j)} = \mathcal{I} - N_j - n_j \tau, & j = 0, \ldots, q-d-1 \end{array} \tag{31}$$

where

$$N_i = \sum_{j=1}^{i} \delta_{j+1} n_{i-j}. \tag{32}$$

The integers n_i are constrained, recursively, by the inequalities

$$\lceil -u_{+}^{(d+i)} + \lambda N_i \rceil \leq n_i \leq \lceil -u_{-}^{(d+i)} + \lambda N_i \rceil, \tag{33}$$

where $u_{+}^{(k)}$ (resp. $u_{-}^{(k)}$) is the sum of all positive (resp. negative) components of $\mathbf{u}^{(k)}$. Furthermore for all $\mathbf{z} \in \mathbf{Z}^2$ such that $\mathcal{E}(\mathbf{z}) \in \Omega_{\mathbf{n}}$, we have

$$\mathbf{v}(\mathbf{z}) = (a,\, b) \qquad a = \sum_{j=1}^{q-d} \delta_{j+1} n_{q-d-j}, \qquad b = \sum_{j=2}^{q-d} \delta_{j+2} n_{q-d-j}. \tag{34}$$

We note that one of the $\Omega_{\mathbf{n}}$ of proposition 3.1 is always degenerate (dimension $< d$), namely the case $n_i = 0$, $i = 0, \ldots, q-d-1$. This corresponds to the unique fixed point of Φ at the origin.

Proof of theorem 2. That the $\Omega_{\mathbf{n}}$ are convex polyhedra corresponding to level sets of the vector field is part of proposition 3.1, to be proved below. By definition ([4], Chapter IV), uniform distribution implies the equivalence of density in $\mathbf{Z}^2$ and normalized volume in Ω for any finite collection of elementary sets (parallelepipeds with sides parallel to the coordinate axes). To extend this correspondence to the polyhedra $\Omega_{\mathbf{n}}$, we note that the boundary of $\bar{\Omega}_{\mathbf{n}}$ is a compact set of zero Lebesgue measure, and so for every $\epsilon > 0$, it admits a *finite* cover $\mathcal{B}_\epsilon$ of elementary sets, of total measure less than ϵ. But then the complement of $\mathcal{B}_\epsilon$ in $\bar{\mathcal{L}}$ is also a finite family of elementary sets, each contained in either $\bar{\Omega}_{\mathbf{n}}$ or its complement (not both, lest $\mathcal{B}_\epsilon$ would not cover their common boundary). Thus $\bar{\Omega}_{\mathbf{n}}$ contains a finite (possibly empty) collection of elementary sets whose measure differs from that of $\bar{\Omega}_{\mathbf{n}}$ by at most ϵ. Since ϵ was arbitrary, our result follows. $\square$

To prove proposition 3.1, we first need a lemma

Lemma 3.2 *The following holds*

$$\begin{aligned} C\cdot \mathbf{e}^{(t)} &\equiv \mathbf{e}^{(t-1)}\,(\mathrm{mod}\ \tau), \qquad t=-1,\ldots,d-1. \\ C\cdot \mathbf{e}^{(-2)} &\equiv -\mathbf{e}^{(-1)}\,(\mathrm{mod}\ \tau) \end{aligned}$$

Proof. Since the matrix C shifts all coordinates except the last one, we only need to look at the $(d-1)$th component of the above congruences. We begin with the first congruence. From (14) and (11) we have, for the last component

$$C\,\mathbf{e}^{(t)}_{d-1} = -\mathbf{c}\cdot\mathbf{e}^{(t)} \equiv \mathbf{e}^{(t-1)}_{d-1} = \delta_{d-t-1}\,(\mathrm{mod}\ \tau). \tag{35}$$

Let t be odd, $t = d-2\,i+1$. Equations (21) and (12) give

$$-\mathbf{c}\cdot\mathbf{e}^{(d-2\,i-1)} \equiv (-1)^{i+1}\,(\mathrm{mod}\ \tau) \qquad\qquad \mathbf{e}^{(d-2\,i)}_{d-1} = \delta_{2\,i-2} = (-1)^{i-1},$$

as desired. Likewise, for $t = d-2\,i$, even

$$-\mathbf{c}\cdot\mathbf{e}^{(d-2\,i)} \equiv 0\,(\mathrm{mod}\ \tau) \qquad\qquad \mathbf{e}^{(d-2\,i)}_{d-1} = \delta_{2\,i-1} = 0.$$

Similarly, for the remaining congruence

$$C\,\mathbf{e}^{(-2)}_{d-1} = -\mathbf{c}\cdot\mathbf{e}^{(-2)} \equiv 0\,(\mathrm{mod}\ \tau) \qquad\qquad -\,\mathbf{e}^{(-1)}_{d-1} = \delta_{d-3} = 0$$

which completes the proof. □

Proof of proposition 3.1

By construction, the first d vectors $\mathbf{u}^{(i)}$ are just unit vectors (30), which, for any ζ in $\Omega = \mathcal{I}^d$, gives

$$\zeta_i = \mathbf{u}^{(i)}\cdot\zeta \,\in \mathcal{I} \tag{36}$$

and we have the first d pairs of bounds. Application of (16) gives

$$\Phi^*(\zeta) = C\cdot\zeta - n_0\,\mathbf{e}^{(d-1)} = (\zeta_1,\ldots,\zeta_{d-1},-\mathbf{c}\cdot\zeta + n_0\tau),$$

and thus

$$\mathbf{u}^{(d)}\cdot\zeta = (C'\cdot\mathbf{u}^{(d-1)})\cdot\zeta \,\in \mathcal{I} - n_0\tau. \tag{37}$$

Since the c_i are constants and $|\zeta_i| < \tau$, the integer n_0 can take on a finite number of values. The region Ω is thus partitioned into a finite number of convex sub-regions

Ω_{n_0}, with boundaries specified by (36) and (37). Similarly, a second application of Φ^* gives

$$(\Phi^*)^2(\zeta) = C^2 \cdot \zeta - n_0\,\mathbf{e}^{(d-2)} - n_1\mathbf{e}^{(d-1)},$$

where $n_1 \in \mathbf{Z}$ is again one of a finite number of integers such that $(\Phi^*)^2(\zeta)_{d-1} \in \mathcal{I}$. Here we have used lemma (3.2). For fixed n_0 and n_1, we have, from (30)

$$\mathbf{u}^{(d+1)} \cdot \zeta = (C' \cdot \mathbf{u}^{(d)}) \cdot \zeta \in \mathcal{I} + n_0 - n_1\tau.$$

Thus $\Omega = \bigcup_{n_0,n_1} \Omega_{n_0,n_1}$, where the action of Φ^* on Ω_{n_0,n_1} is an inhomogeneous linear transformation labeled by n_0, n_1. Continuing in this way, we obtain the bounding intervals in the statement of the proposition. The final iteration yields a partition $\Omega = \bigcup_{\mathbf{n}} \Omega_{n_0 \ldots n_{q-d-1}}$, with

$$\begin{aligned}(\Phi^*)^q\zeta = C^q\zeta \quad &+ \quad (-n_{q-d-1} + n_{q-d-3} + \cdots\,)\,\mathbf{e}^{(-1)} \\ &+ \quad (-n_{q-d-2} + n_{q-d-4} + \cdots\,)\,\mathbf{e}^{(-2)} \\ &+ \quad \sum_{t=0}^{d-1} n_{q-d+t}\,\mathbf{e}^{(t)}.\end{aligned}$$

But C^q is the identity, so the coefficients of $\mathbf{e}^{(-1)}$ and $\mathbf{e}^{(-2)}$ in the above expression for $(\Phi^*)^q$ differ from those of ζ by a and b of (34). Thus all $\zeta \in \Omega_{\mathbf{n}}$ correspond to the same vector field (a, b) given by (34).

It remains to establish the inequalities (33). We do this assuming $\tau > 0$; the derivation for $\tau < 0$ differs only in minor details. From (31), we have

$$N_i - \lambda\mathbf{u}^{(d+i)} \cdot \zeta \leq n_i < 1 + N_i - \lambda\mathbf{u}^{(d+i)} \cdot \zeta.$$

Using

$$\sup_{\zeta\in\Omega} \lambda\mathbf{u}^{(k)} \cdot \zeta = u_+^{(k)} \qquad\qquad \inf_{\zeta\in\Omega} \lambda\mathbf{u}^{(k)} \cdot \zeta = u_-^{(k)},$$

and recalling that n_i is an integer, we get the claimed result. □

In Section 4 we shall discuss the localization of arbitrary phase-space trajectories (periodic orbits). This will involve a recursive partition of the sets $\Omega_{\mathbf{n}}$, exploiting the following important corollary of Theorem 2.

Proposition 3.3 *Let $S \subseteq \Omega_{\mathbf{n}}$ be any convex polyhedron defined by the conditions*

$$\mathbf{u}^{(i)} \cdot \zeta \in \mathcal{I}^{(i)}(S), \qquad i = 1, \ldots, q-1$$

where $\mathcal{I}^{(i)}(S)$ is a half-open real interval with endpoints in $\mathcal{M}[1,\tau]$, open to the right (resp. left) for $\lambda > 0$ (resp. $\lambda < 0$). Then the map Φ^* acts on S by cyclically permuting the bounds and then translating them:

$$\mathcal{I}^{(i)}(\Phi^*(S)) = \mathcal{I}^{(i+1\ (\mathrm{mod}\ q))}(S) + n_0\, \mathbf{u}^{(i)} \cdot \mathbf{e}^{(d-1)}.$$

The density of the points in $\mathbf{Z}^2$ whose local image lies in S is equal to normalized volume of S, which is an algebraic number in $\mathbf{Q}(\lambda)$.

Proof. From theorem (1) and the identity

$$C'\mathbf{u}^{(q-1)} = (C')^q \mathbf{u}^{(0)} = \mathbf{u}^{(0)}$$

we have

$$\mathbf{u}^{(i)} \cdot \Phi^*(\zeta) = \mathbf{u}^{(i+1) \bmod q} \cdot \zeta - n_0 \mathbf{u}^{(i)} \cdot \mathbf{e}^{(d-1)}. \tag{38}$$

The result follows from the assumed bounds on $\mathbf{u}^{(i)} \cdot \zeta$. □

We conclude this section by presenting an alternative q-dimensional representation of the local mapping, which is in the spirit of the embedding techniques developed for web maps, see e.g., [13, 8].

Proposition 3.4 *The mapping $\mathcal{F} : \Omega \to \mathbf{R}^q$ defined coordinate-wise by*

$$\mathcal{F}(\zeta)_i = \mathbf{u}^{(i)} \cdot \zeta, \qquad i = 0, \ldots, q-1 \tag{39}$$

conjugates Φ^* on Ω to a cyclic permutation of coordinates followed by a translation. Specifically, for all $\bar{\zeta} \in \mathcal{F}(\Omega)$.

$$\mathcal{F} \circ \Phi^* \circ \mathcal{F}^{-1}(\bar{\zeta})_i = \bar{\zeta}_{(i+1) \bmod q} - n_0 \mathbf{u}^{(i)} \cdot \mathbf{e}^{(d-1)}. \tag{40}$$

Proof. The inverse of $\mathcal{F}$ is well-defined, since

$$\bar{\zeta}_i = \mathcal{F}(\zeta)_i = \zeta_i, \qquad i = 0, \ldots, d-1.$$

From theorem (1), we must calculate

$$\mathcal{F}(C \cdot \zeta - n_0 \mathbf{e}^{(d-1)}).$$

Substituting from (39) this is

$$\begin{aligned} C'\mathbf{u}^{(i)} \cdot \zeta - n_0 \mathbf{u}^{(i)} \cdot \mathbf{e}^{(d-1)} &= \mathbf{u}^{(i+1) \bmod q} \cdot \zeta - n_0\, \mathbf{u}^{(i)} \mathbf{e}^{(d-1)} \\ &= \bar{\zeta}_{(i+1) \bmod q} - n_0\, \mathbf{u}^{(i)} \cdot \mathbf{e}^{(d-1)}. \end{aligned}$$

□

4 Local periodic orbits

Proposition 3.3 provides the basis for a systematic construction of the periodic orbits of the round-off model. Here we use the word 'orbit' to refer to an equivalence class of orbits of Φ which are translate of one another, that is, which share the same vector-field sequence.

We now describe an algorithm for finding all orbits of period less than or equal to some cut-off N. Initial conditions for the entire equivalence class lie in a convex polyhedron S with q bounding intervals $\mathcal{I}^{(i)}(S)$ as in the statement of proposition 3.3.

The polyhedron $\Phi^*(S)$ is calculated using Proposition 3.3. The full algorithm is an extension of the technique used to obtain the partition $\Omega = \bigcup_{\mathbf{n}} \Omega_{\mathbf{n}}$ of Theorem 2. Such partition provides the lowest level (level 0) of a recursive algorithm.

We assign an arbitrary order to the $\Omega_{\mathbf{n}}$, renaming them $\Omega_{i_0}, i_0 = 0, 1, 2, \ldots$. For each i_0, in order, we shall collect all periodic orbits of period not exceeding N which pass through Ω_{i_0} but which avoid all of the Ω_{j_0} with $j_0 < i_0$ (to avoid multiple counting). As a first step in the systematic search, we construct the *transition matrix*, i.e., we list, for each i_0, the set of j_0 such that $\Phi^*(\Omega_{i_0}) \cap \Omega_{j_0} \neq \emptyset$. For level 0, the number of such j_0 is either one (no branching) or two (branching). Periodic orbits at level 0 correspond to those Ω_{i_0} such that $\Phi^*(\Omega_{i_0}) = \Omega_{i_0}$, with Φ^{*q} acting as the identity on Ω_{i_0}. We store these orbits and delete the corresponding rows and columns of the transition matrix. After we have completed the search for periodic orbits originating in Ω_{i_0}, we delete its row and column as well.

For each non-periodic Ω_{i_0}, we proceed with the search for periodic orbits by determining the *first-return map* for Ω_{i_0}, i.e., we construct the partition

$$\Omega_{i_0} = \bigcup_{i_1} \Omega_{i_0 i_1} \cup \Omega_{i_0}^{\infty},$$

where each $\Omega_{i_0 i_1}$ is a convex polyhedron such that

$$\Phi^{*n_{i_0 i_1}}(\Omega_{i_0 i_1}) \subset \Omega_{i_0},$$

and $n_{i_0 i_1}$ is the smallest positive integer with this property. The remainder $\Omega_{i_0}^{\infty}$ is defined by the condition

$$\Phi^{*n}(\Omega_{i_0}^{\infty}) \cap \Omega_{i_0} = \emptyset \qquad 1 \leq n \leq N,$$

hence contains no points in orbits of period $\leq N$. For each $\Omega_{i_0 i_1}$, we store, not only the endpoints of the intervals $\mathcal{I}^{(i)}(\Omega_{i_0 i_1})$, but also the return time $n_{i_0 i_1}$ and the translation vector $\chi_{i_0 i_1}$ associated with the action of $\Phi^{*n_{i_0 i_1}}$ via iterated application of Proposition 3.3,

$$\mathcal{I}^{(k)}(\Phi^{*n_{i_0 i_1}}(\Omega_{i_0 i_1})) = \mathcal{I}^{(k+n_{i_0 i_1} \pmod{q})}(\Omega_{i_0 i_1}) + \chi_{i_0 i_1}.$$

To find the $\Omega_{i_0 i_1}$, we start with Ω_{i_0} and apply Φ^* iteratively. At each step we intersect the image region with each of the Ω_{j_0} having a non-empty entry in the relevant row of the transition matrix. If S is any one of the resulting regions, we have three alternatives. If the accumulated number of iterations exceeds N, we include S in $\Omega_{i_0}^{\infty}$. Otherwise, if S is contained in Ω_{i_0}, corresponding to a first return, we append its preimage to the set of $\Omega_{i_0 i_1}$. If neither of these conditions apply, we continue the iteration. This is obviously a finite branching process which must end in the desired partition of Ω_{i_0}. In this way we reach level 1 of a recursive process, which at level L produces a collection of convex polyhedra $\Omega_{i_0 \cdots i_L}$, each specified by its $2q$ bounds and equipped with a return time $n_{i_0 \cdots i_L}$ and a translation vector $\chi_{i_0 \cdots i_L}$. The recursion $\mathcal{R}$ from level L to level $L+1$ can be summarized as follows:

Step 1. Construct the level-L transition matrix, i.e., for each i_L, list all j_L such that

$$\Phi^{*n_{i_0 \cdots i_L}}(\Omega_{i_0 \cdots i_L}) \cap \Omega_{i_0 \cdots i_{L-1} j_L} \neq \emptyset.$$

Step 2. Using the transition matrix, identify all $\Omega_{i_0 \cdots i_L}$ such that

$$\Phi^{*n_{i_0 \cdots i_L}}(\Omega_{i_0 \cdots i_L}) = \Omega_{i_0 \cdots i_L}.$$

From these extract the periodic regions, storing their bounds and first-return times, and removing the corresponding rows and columns from the transition matrix.

Step 3. For each i_L, with non-periodic $\Omega_{i_0\cdots i_L}$

(i) construct the first-return map and corresponding partition

$$\Omega_{i_0\cdots i_L} = \bigcup_{i_{L+1}} \Omega_{i_0\cdots i_{L+1}} \cup \Omega^{\infty}_{i_0\cdots i_L},$$

storing the bounds, return time, and translation vector for each $\Omega_{i_0\cdots i_{L+1}}$;

(ii) apply $\mathcal{R}$ on $\{\Omega_{i_0\cdots i_{L+1}},\, i_{L+1} = 0, 1, \ldots\}$;

(iii) delete row i_L and column i_L from the level-L transition matrix.

Step 4. Exit level L. If $L = 0$, the process terminates.

Because of the contraction of the transition matrix, exhaustive application of $\mathcal{R}$ stores the data for one convex polyhedron for each distinct sequence of level-0 regions visited by an orbit. If the polyhedron has a return time n, then there are n mutually congruent polyhedra in Ω corresponding to Φ^* orbits of period $n' = \mathrm{lcm}(n, q)$. Of these, the process $\mathcal{R}$ identifies and stores one and only one.

5 Applications to a cubic case

We apply the algorithm described in the previous section to the case $q = 7$. This is the smallest value of q for which the trace of the round-off mapping is an algebraic integer of degree three (figure 1).

The parameter λ is one of the three roots of the polynomial

$$h_7(x) \;=\; x^3 + x^2 - 2x - 1$$

namely,

$$\lambda = 2\cos\frac{2k\pi}{7}, \qquad k = 1, 2, 3.$$

Since $\phi(7) = 6$, the dimension of the local space is $d = 4$. The basis (11) becomes

$$\begin{aligned}
\mathbf{e}^{(-2)} &= (\;\;0, -1, \;\;0, \;\;1)\\
\mathbf{e}^{(-1)} &= (\;\;1, \;\;0, -1, \;\;0)\\
\mathbf{e}^{(0)} &= (-\tau, \;\;1, \;\;0, -1)\\
\mathbf{e}^{(1)} &= (\;\;0, -\tau, \;\;1, \;\;0)\\
\mathbf{e}^{(2)} &= (\;\;0, \;\;0, -\tau, \;\;1)\\
\mathbf{e}^{(3)} &= (\;\;0, \;\;0, \;\;0, -\tau)
\end{aligned}$$

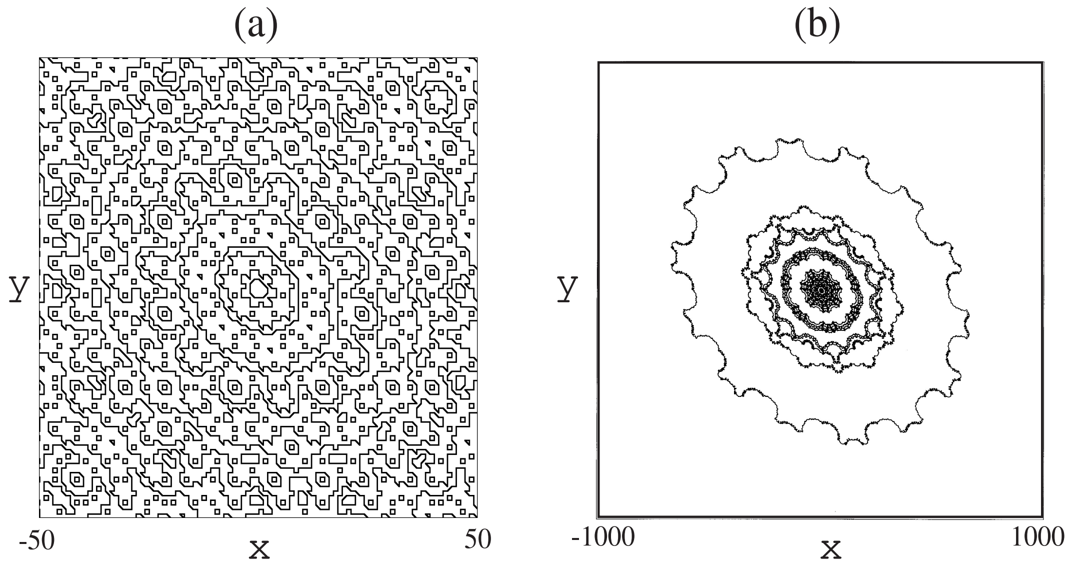

Figure 3: Orbits for the rotation number 2/7. (a) all orbits in the region $-50 \leq x, y \leq 50$ excluding the fixed points, where the vector field (5) vanishes. Orbits which surround the origin (annular orbits) are unique, while all others are repeated quasi-periodically over the entire plane. (b) all annular orbits lying entirely in the region $-1000 \leq x, y \leq 1000$.

and the matrix (14) implementing the round-off map in the local hypercube Ω is, from (19),

$$\mathbf{C} = \begin{pmatrix} 0 & 1 & 0 & 0 \\ 0 & 0 & 1 & 0 \\ 0 & 0 & 0 & 1 \\ -1 & -\lambda - 1 & -\lambda^2 - \lambda & -\lambda - 1 \end{pmatrix}.$$

We have carried out the systematic search for periodic orbits described in Section 4 for the rotation numbers 1/7 (approximately 10^6 orbit classes of period ≤ 21000) and 2/7 (approximately $6 \cdot 10^5$ orbit classes of period ≤ 49000). We present details only of the second case, which has a simpler vector field.

To begin the search, we determined the level-0 regions which partition Ω. The boundaries are determined by the equations (31) for $\zeta = (\zeta_0, \zeta_1, \zeta_2, \zeta_3)$

$$\zeta_k = \mathcal{I}, \qquad i = 0,1,2,3; \qquad \begin{array}{ll} u^{(4)} \cdot \zeta & \in \mathcal{I} - n_0\tau, \\ u^{(5)} \cdot \zeta & \in \mathcal{I} - n_1\tau + n_0, \\ u^{(6)} \cdot \zeta & \in \mathcal{I} - n_2\tau + n_1 \end{array}$$

where

$$\begin{aligned} u^{(4)} &= (-1,\, -\lambda-1,\, -\lambda^2-\lambda,\, -\lambda-1), \\ u^{(5)} &= (\lambda+1,\, \lambda^2+2\lambda,\, \lambda^2+2\lambda,\, \lambda+1), \\ u^{(6)} &= (-\lambda-1,\, -\lambda^2-\lambda,\, -\lambda-1,\, -1) \end{aligned}$$

and $\mathcal{I} = (\tau,\, 0]$.

There are 17 nonempty convex polyhedra satisfying the bounds (5) and we list their data in the table below. These polyhedra feature to 9 distinct values of the vector field $\mathbf{v} = (a, b)$ (cf. equation (34)).

region	n_0	n_1	n_2	a	b	measure $\times$ 24
0	0	0	0	0	0	0
1	0	1	0	0	-1	$-1-2\lambda+2\lambda^2$
2	0	1	1	0	-1	$2+\lambda-3\lambda^2$
3	1	-1	2	-1	-1	$1-\lambda-\lambda^2$
4	1	0	0	1	0	$-1-2\lambda+2\lambda^2$
5	1	0	1	0	0	$159-33\lambda-74\lambda^2$
6	1	0	2	-1	0	$84-17\lambda-32\lambda^2$
7	1	1	0	1	-1	$46+58\lambda+16\lambda^2$
8	1	1	1	0	-1	$45-99\lambda-65\lambda^2$
9	1	1	2	-1	-1	$-\lambda-2\lambda^2$
10	2	-1	1	1	1	$2+\lambda-3\lambda^2$
11	2	-1	2	0	1	$84-17\lambda-32\lambda^2$
12	2	-1	3	-1	1	$5-26\lambda-16\lambda^2$
13	2	0	1	1	0	$45-99\lambda-65\lambda^2$
14	2	0	2	0	0	$129+95\lambda+13\lambda^2$
15	2	1	1	1	-1	$-\lambda-2\lambda^2$
16	3	-1	2	1	1	$-\lambda-2\lambda^2$

One verifies that the volumes add up, as they must, to the total volume τ^4 of the local phase space. The respective normalized volumes give the densities of the points in each equivalence class.

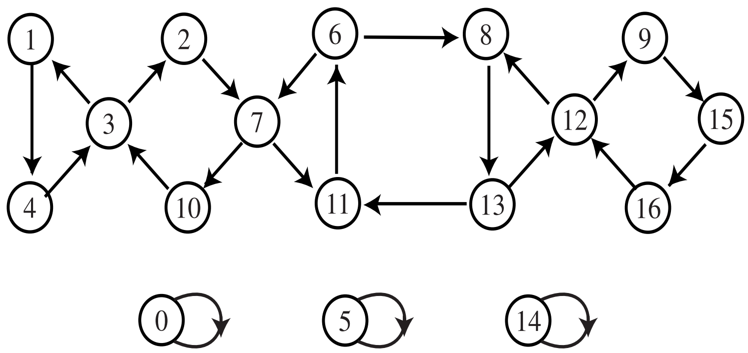

Figure 4: The graph of the level-0 transition matrix. Each vertex of the graph represents the corresponding numbered region listed in the table. Under the action of the map Φ^*, each level-0 region is mapped into the union of at most two regions, as represented by the oriented edges of the graph. In three cases, the region is mapped into itself, corresponding to periodic orbits of period 1 (region 0) or period 7 (regions 5 and 14). These are the isolated vertices in the graph.

The transition matrix for level 0 is displayed in Fig. 4 in the form of a graph. If the image of region i intersects region j, then the graph contains an oriented edge from vertex i to vertex j. Each vertex has either one or two outgoing edges.

Orbits of Φ^7 are displayed in figures 1 and 3. Fig. 1, gives an overview of the structure of the phase space surrounding the origin. For clarity, we display only the orbits of sufficiently large period (≥ 200). A more detailed view of the innermost region is shown in Fig. 3a, which features all orbits except the fixed points. The latter correspond to the points where the discrete vector field (5) vanishes. Orbits which surround the origin (annular orbits) are unique, while all others are repeated quasi-periodically over the entire plane. Whereas the annular orbits are associated with isolated points in the local hypercube, the rest correspond to 4-dimensional convex polyhedra. A selected set of annular orbits is depicted in Fig. 3b.

Following the algorithm sketched in Section 4, we employed an efficient C program to collect data on all periodic orbits with period not exceeding 49000. We identified a total of 629159 distinct orbit classes, accounting for more than 97% of the total measure. The calculation required about seven days of CPU time using a

400 MHz Pentium II processor[2].

Having listed the geometrical and dynamical data for all orbit classes γ with period $T(\gamma)$ not exceeding $N = 49000$, we calculate their density measure $\mu(\gamma)$ by computing the 4-dimensional normalized volume of the corresponding polyhedron, multiplied by the number of local-space translates linked by the map, i.e., the return time $R(\gamma)$. For all orbits with non-vanishing $\mu(\gamma)$, we have

$$T(\gamma) = \begin{cases} R(\gamma) & \text{if } R(\gamma) \equiv 0 \pmod 7 \\ 7R(\gamma) & \text{otherwise.} \end{cases}$$

We are now in a position to calculate the fraction of the total density measure accounted for by the orbits with $T(\gamma) \leq N$, namely

$$\mu(T(\gamma) \leq N) = \sum_{\gamma : T(\gamma) \leq N} \mu(\gamma) \simeq 0.97$$

as well as a good approximation to the probability distribution for the propagation of round-off errors for times $t \ll N$. Specifically we have

$$P(\mathbf{z}, t) = \sum_{\gamma} \mu(\gamma) \Pi_{\gamma}(\mathbf{z}, t)$$

where $\Pi_{\gamma}(\mathbf{z}, t)$ is the fraction of points of γ displaced on $\mathbf{Z}^2$ by $\mathbf{z}$ after t iterations of Φ^7.

We carried out the above procedure to calculate $P(\mathbf{z}, t)$ for $t = 100$. The result is displayed in figure 5. Averaging over a large number of orbit classes has resulted in a probability distribution which differs markedly from that of the rotation number 1/5 (see [9], figure 2), where for comparable values of t, $P(\mathbf{z}, t)$ can be analyzed into contributions from a small number of nearly self-similar orbits. At the same time, $P(\mathbf{z}, t)$ is also quite different from what one would expect from a random walk on a lattice, showing considerably more radial and angular correlations.

To calculate $\Pi_{\gamma}(\mathbf{z}, t)$ it is not necessary to know the location of a representative $\mathbf{Z}^2$ trajectory in the equivalence class of the orbit γ (in fact, finding such representative for large-period γ would be prohibitively time-consuming). Instead, one can start with the polyhedron representing γ and iterate the local map using Proposition 3.3 to generate the sequence of vector fields. This is all we need to determine systematically the displacement vector $\mathbf{z}$ for each iteration time $7t$.

[2]The C source files are available at `http://poincare.physics.nyu.edu/~jhl2/Orbiter[2_7]`

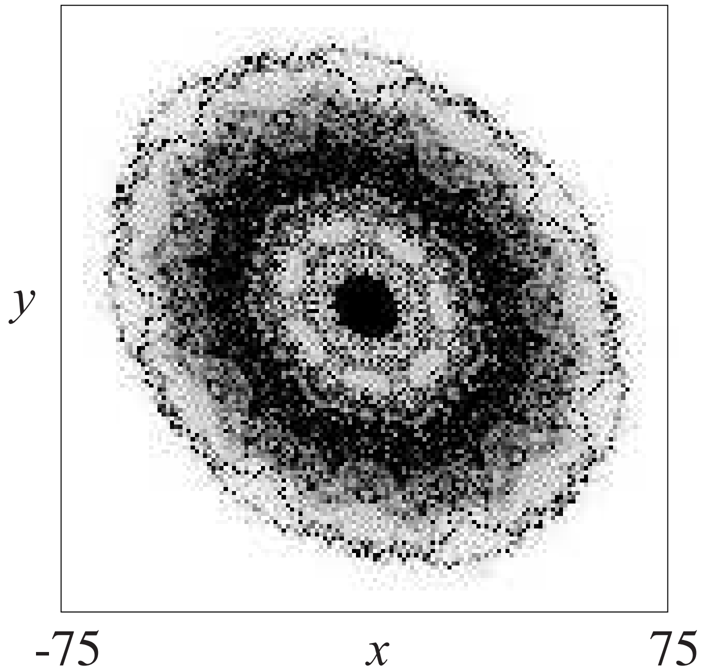

Figure 5: Probability distribution for the propagation of round off errors after 100 iterates of the composed map Φ^7, computed using 97.4% of the total measure. Each displacement on the integer lattice in the range $-75 \leq x, y \leq 75$ is assigned one of 256 gray levels varying from 0 (white) to 255 (black). The (0,0) displacement has an exceptionally large probability of .6733 and is assigned gray level 255. Every other displacement has a probability between 0 to .00401, and is assigned a gray level proportional to its probability.

Based on preliminary numerical data on several rotation numbers p/q, there appears to be a fundamental qualitative distinction between the round-off models with quadratic irrational λ —of which $q = 5$ is the simplest example— and the cases of λ of higher degree. Although all of these models are non-chaotic (zero metric entropy), the non-quadratic cases clearly display a considerably higher level of complexity, as we have seen in the qualitative behavior of the round-off error propagation for $q = 7$.

A natural observable is the number $\nu(T)$ of orbit classes of minimal Φ^q-period T. In the quadratic cases we have studied so far, the orbits with non-zero density are members of a small number of scaling families with the the periods T_n increasing exponentially for large n within each family. As a result, $\nu(T)$ is equal to zero for all but an exponentially sparse set of T values, for which $\nu(T) = 1$).

The behaviour of the multiplicity function $\nu(T)$ for $q = 7$ is strikingy different from those of the quadratic λ-cases. Specifically, $\nu(T)$ appears to be non-zero for all but finitely many values of T, and to be slowly increasing, on average, with increasing T. The multiplicity function for $p/q = 7$, and $T \leq 7000$ was calculated from our numerical data, and is shown in figure 2.

References

[1] R . Adler, B. Kitchens and C. Tresser, Dynamics of nonergodic piecewise affine maps of the torus, Preprint, IBM, Yorktown Heights, NY 10598, (1999).

[2] M. Blank, Pathologies generated by round-off in dynamical systems, *Physica D* **78** (1994) 93–114.

[3] D. Bosio and F. Vivaldi, Round-off errors and p-adic numbers, *Nonlinearity* **13** (2000) 309–322.

[4] J. W. S. Cassels, *An introduction to diophantine approximations*, Cambridge University Press, Cambridge (1957).

[5] P. Diamond, P. Kloeden, V. Kozyakin and A. Pokrovskii, Boundedness and dissipativity of truncated rotations on uniform planar lattices, Preprint TR M95/06, School of Computing and Mathematics, Deaking University, Geelong, Vic., Australia (1995).

[6] R. Lidl and H. Niederreiter, *Introduction to finite fields and their applications*, Cambridge University Press, Cambridge (1986).

[7] J. H. Lowenstein, S. Hatjispyros and F. Vivaldi, Quasi-periodicity, global stability and scaling in a model of Hamiltonian round-off, *Chaos* **7** (1997) 49–66.

[8] J. H. Lowenstein, Fixed-point densities for a quasiperiodic kicked-oscillator map, *Chaos* **5** (1995) 566–577.

[9] J. H. Lowenstein and F. Vivaldi, Anomalous transport in a model of hamiltonian round-off errors, *Nonlinearity* **11** (1998) 1321–1350

[10] P. J. McCarthy, *Algebraic extensions of fields*, Dover, New York (1991).

[11] F. Vivaldi, Periodicity and transport from round-off errors, *Experimental Mathematics* **3** (1994) 303–315.

[12] I. Vladimirov, Discretization of dynamical systems, preprint, Deakin University, Geelong, Victoria. (1996). [`I.Vladimirov@mailbox.uq.edu.au`]

[13] G. M. Zaslavskii, R. Z. Sagdeev, D. A. Usikov, and A. A. Chernikov, *Usp. Fiz Nauk* **156** (1988) 193. [*Sov. Phys. Usp.* **31** (1988)